Acta Cryst. (1977). A33, 146–150

Lattice Dynamics, Thermal Expansion and Bulk Modulus of Erbium

BY R. RAMJI RAO AND A. RAMANAND

Department of Physics, Indian Institute of Technology, Madras 600036, *India*

(*Received* 29 *April* 1976; *accepted* 27 *July* 1976)

The lattice dynamics and the temperature variation of the volume Grüneisen function and bulk modulus of erbium have been calculated with the nearest-neighbour central-interaction model of Srinivasan & Ramji Rao [*Inelastic Scattering of Neutrons*, IAEA, Vienna, (1965), **1**, 325–342]. The even moments of the frequency distribution function of erbium have also been calculated. The agreement between the calculated $\bar{\gamma}_H$ and that obtained from thermal data is good. The calculated B_S values agree with those obtained from the measured elastic constants of Fisher & Dever [*Trans. Metall. Soc. AIME*, (1967), **239**, 48–57] at various temperatures up to 298 K, to within 2%.

1. Introduction

Erbium is a hexagonal rare-earth metal with a c/a ratio of 1·573. The second-order elastic (SOE) constants of Er from 81 to 298 K were measured by Fisher & Dever (1967). Fisher, Manghnani & Kikuta (1973) measured the SOE constants and the pressure derivatives of Er at 298 K. Gschneidner (1964) reported a value of 1·17 for the thermal γ_H of Er. Ramji Rao & Menon (1973) calculated the lattice dynamics and thermal expansion of Er using Keating's (1966) approach. Ramji Rao (1975*a*) calculated the third-order elastic (TOE) constants and pressure derivatives of the SOE constants of Er at 298 K using the nearest-neighbour central-force model (C.F. model) of Ramji Rao & Srinivasan (1968, 1969). The object of the present paper is to calculate the thermal expansion and lattice dynamics of Er with the C.F. model of Srinivasan & Ramji Rao (1965). The Anderson–Grüneisen (A–G) parameter, δ, of Er has been evaluated from the calculated TOE constants of the C.F. model by the procedure suggested by Ramji Rao (1974). The bulk moduli of Er at various temperatures have been evaluated using Anderson's (1966) theory and compared with those obtained from the experimental elastic constants data of Fisher & Dever (1967).

2. Lattice dynamics

The normal mode frequencies of the lattice vibrations are obtained as solutions of the determinant equation:

$$\left| \begin{bmatrix} k & k' \\ i & j \end{bmatrix}^{\mathbf{q}} - \omega^2 \delta_{kk'} \delta_{ij} \right| = 0; \qquad (2.1)$$

$\begin{bmatrix} k & k' \\ i & j \end{bmatrix}^{\mathbf{q}}$ are the coupling coefficients of the dynamical matrix. The expressions for the coupling coefficients of a homogeneously deformed ideal h.c.p. lattice with nearest-neighbour central interaction were evaluated by Srinivasan & Ramji Rao (1965). The central interaction potential has the form:

$$\Phi(r) = -\frac{a}{r^m} + \frac{b}{r^n}. \qquad (2.2)$$

Fig. 1(*a*) and (*b*) shows the theoretical dispersion curves in the [0001] and [01$\bar{1}$0] directions for Er. The

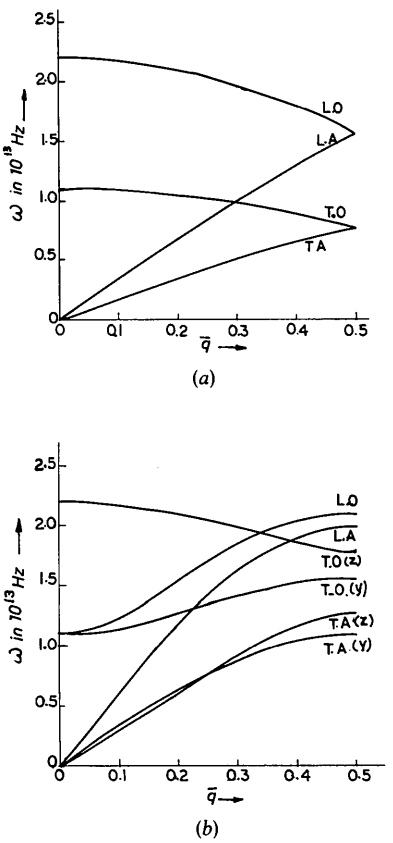

Fig. 1. (*a*) Theoretical dispersion curves for erbium in the [0001] direction. (*b*) Theoretical dispersion curves for erbium in the [01$\bar{1}$0] direction.

experimental dispersion relations for erbium are not available in the literature. However, the neutron inelastic scattering measurements of the phonon dispersion relations of terbium and holmium were made by Glyden Houman & Nicklow (1970) and Nicklow, Wakabayashi & Vijayaraghavan (1971) respectively. To make a comparison, the lattice frequencies of Er at the zone centre (Γ) and the zone boundaries (A and M) are obtained by extrapolating the experimental frequencies of Tb and Ho. This is a reasonable surmise as these rare-earth metals belong to the same group. The lattice frequencies calculated on the present model agree well with the extrapolated values. The calculated and extrapolated frequencies of Er together with the experimental frequencies of Tb and Ho in the [0001] and [01$\bar{1}$0] symmetry directions are given in Table 1. The maximum discrepancy between the calculated and extrapolated values in the [0001] direction occurs for the Γ_6^- frequency and is about 12%. In the [01$\bar{1}$0] direction the maximum discrepancy between the calculated and extrapolated frequencies is 8% and this occurs for M_2^- and M_3^+ frequencies. The general pattern of the dispersion curves of Er conforms with that of the other hexagonal metals. The frequencies of Er obtained by Ramji Rao & Menon (1973) using Keating's (1966) approach are higher than the frequencies obtained on the C.F. model.

Table 1. *The experimental frequencies of terbium and holmium and the extrapolated and calculated frequencies of erbium in the* [0001] *and* [01$\bar{1}$0] *directions*; ω *in* 10^{13} Hz

(*a*) [0001] direction

	LO (Γ_3^+)	LO and LA (A_1)	TO (Γ_6^-)	TO and TA (A_3)
Tb	2·042	1·533	1·144	0·817
Ho	2·136	1·609	1·219	0·842
Er (extrapolated)	2·180	1·646	1·257	0·855
Er (calculated)	2·202	1·557	1·101	0·778

(*b*) [01$\bar{1}$0] direction

	LO (M_2^-)	LA (M_1^+)	TA(Y) (M_4^+)	TO(Z) (M_3^+)	TA(Z) (M_4^-)
Tb	1·916	1·822	0·999	1·816	1·100
Ho	1·935	1·910	1·037	1·916	1·232
Er (extrapolated)	1·945	1·955	1·056	1·967	1·298
Er (calculated)	2·108	2·010	1·101	1·798	1·271

3. Thermal expansion

We now define the generalized Grüneisen parameters (G.P.'s) for the normal-mode frequencies of a hexagonal crystal.

$$\gamma'(\omega) = -\frac{1}{\omega}\frac{\partial\omega}{\partial\varepsilon'},$$
$$\gamma''(\omega) = -\frac{1}{\omega}\frac{\partial\omega}{\partial\varepsilon''}. \tag{3.1}$$

Here ε' is a uniform areal strain perpendicular to the hexagonal axis and ε'' is a uniform longitudinal strain parallel to the hexagonal axis. The effective Grüneisen function $\bar{\gamma}^1(T)$ is defined as the weighted average of the individual G.P.'s.

$$\bar{\gamma}_\perp^1(T) = \frac{\sum_{\mathbf{q},j}\gamma'(\mathbf{q},j)C_v(\mathbf{q},j)}{\sum_{\mathbf{q},j}C_v(\mathbf{q},j)},$$
$$\bar{\gamma}_\parallel^1(T) = \frac{\sum_{\mathbf{q},j}\gamma''(\mathbf{q},j)C_v(\mathbf{q},j)}{\sum_{\mathbf{q},j}C_v(\mathbf{q},j)} \tag{3.2}$$

where $\mathbf{q}$ is the wave vector, j is the polarization index and $C_v(\mathbf{q},j)$ is the contribution of a single normal mode of frequency ω to the specific heat of the lattice. The effective Grüneisen functions $\bar{\gamma}^1(T)$ are used to describe the temperature variation of the linear expansion coefficients $\alpha_\perp$ and $\alpha_\parallel$ of the hexagonal crystal.

$$V\alpha_\perp = [(S_{11}+S_{12})\bar{\gamma}_\perp^1(T)+S_{13}\bar{\gamma}_\parallel^1(T)]C_v$$
$$= \bar{\gamma}_\perp^{Br}(T)C_v\chi,$$
$$V\alpha_\parallel = [2S_{13}\bar{\gamma}_\perp^1(T)+S_{33}\bar{\gamma}_\parallel^1(T)]C_v$$
$$= \bar{\gamma}_\parallel^{Br}(T)C_v\chi. \tag{3.3}$$

The effective Grüneisen function $\bar{\gamma}^1(T)$ tends to the limit $\bar{\gamma}^1(0)$ at high temperatures and to the limit $\bar{\gamma}^1(-3)$ at absolute zero. S_{ij} are the elastic compliance coefficients, V is the molar volume and χ is the isothermal compressibility. $\bar{\gamma}_\perp^{Br}(T)$ and $\bar{\gamma}_\parallel^{Br}(T)$ are the average Grüneisen functions used by Brugger & Fritz (1967). From (3.3) we get $\bar{\gamma}_\perp^{Br}$ and $\bar{\gamma}_\parallel^{Br}$ as

$$\bar{\gamma}_\perp^{Br}(T) = \frac{[(S_{11}+S_{12})\bar{\gamma}_\perp^1(T)+S_{13}\bar{\gamma}_\parallel^1(T)]}{\chi},$$
$$\bar{\gamma}_\parallel^{Br}(T) = \frac{[2S_{13}\bar{\gamma}_\perp^1(T)+S_{33}\bar{\gamma}_\parallel^1(T)]}{\chi}. \tag{3.4}$$

At low temperatures the effective Grüneisen functions approach the limits

$$\bar{\gamma}_\perp^1(-3) = \frac{\int\sum_{j=1}^{3}\gamma_j'(\theta,\varphi)V_j^{-3}(\theta,\varphi)\mathrm{d}\Omega}{\int\sum_{j=1}^{3}V_j^{-3}(\theta,\varphi)\mathrm{d}\Omega},$$
$$\bar{\gamma}_\parallel^1(-3) = \frac{\int\sum_{j=1}^{3}\gamma_j''(\theta,\varphi)V_j^{-3}(\theta,\varphi)\mathrm{d}\Omega}{\int\sum_{j=1}^{3}V_j^{-3}(\theta,\varphi)\mathrm{d}\Omega}. \tag{3.5}$$

At low temperature the G.P.'s of the elastic waves determine the anisotropic thermal expansion. $V_j(\theta,\varphi)$ is the wave velocity of the elastic wave of polarization index j propagating in the direction (θ,φ); γ_j' and γ_j'' are the G.P.'s of the acoustic wave. The generalized G.P.'s of the elastic waves can be evaluated from a knowledge of the TOE constants of the material using the procedure suggested by Ramji Rao & Srinivasan (1968, 1970). In the hexagonal crystals, the G.P.'s and the acoustic wave velocities depend only on θ and are independent of the azimuth φ. Table 2 gives the wave velocities and the G.P.'s for the acoustic waves propagating at different angles θ to the Z axis in the X–Z plane. The TOE constants of Er calculated by Ramji Rao (1975*a*) using the C.F. model have been used in evaluating $\bar{\gamma}_L$. The calculated values of $\bar{\gamma}_\perp^1(-3)$ and $\bar{\gamma}_\parallel^1(-3)$ for Er are 0·85 and 0·77 respectively. The low-temperature limits of $\bar{\gamma}_\perp^{Br}$ and $\bar{\gamma}_\parallel^{Br}$ are 0·28 and 0·27 respectively. The low-temperature limit of the volume lattice thermal expansion of Er is given by

$$\bar{\gamma}_L = 2\bar{\gamma}_\perp^{Br}(-3) + \bar{\gamma}_\parallel^{Br}(-3) = 0{\cdot}83\,. \qquad (3.6)$$

Blackman's (1957) procedure is adopted to calculate $\bar{\gamma}^1(T)$ as a function of temperature. A grid of equally spaced points in the irreducible volume of the Brillouin zone is chosen for the wave vector **q**. A program is written for the IBM 370/155 computer to calculate the eigen-frequencies of the dynamical matrix at 84 points evenly distributed over $\frac{1}{24}$ of the volume of the Brillouin zone for the following sets of ε' and ε''.

(1) $\varepsilon'=0, \varepsilon''=0$; (2) $\varepsilon'=0{\cdot}001, \varepsilon''=0$;
(3) $\varepsilon'=-0{\cdot}001, \varepsilon''=0$; (4) $\varepsilon'=0, \varepsilon''=0{\cdot}001$;
(5) $\varepsilon'=0, \varepsilon''=-0{\cdot}001$.

The determinant equation (2.1) is used to calculate the unstrained and the strained frequencies and hence γ' and γ'' for the different lattice wave vectors. The frequencies $\omega(1)$ for the first set of values of ε' and ε'' give the frequencies of the unstrained lattice. The G.P.'s for any frequency are calculated as

$$\gamma' = -\frac{1}{\omega(1)}\frac{[\omega(2)-\omega(3)]}{0{\cdot}002},$$
$$\gamma'' = -\frac{1}{\omega(1)}\frac{[\omega(4)-\omega(5)]}{0{\cdot}002}. \qquad (3.7)$$

The range of frequencies from 0 to ω_{max} is divided into small intervals ($\Delta\omega = 0{\cdot}2\times10^{13}$ Hz) and the number of frequencies in each interval is counted. A histogram is drawn for $g(\omega)$ *versus* ω and is replaced by a smooth curve enclosing unit area with the ω-axis. This gives the normalized frequency distribution curve for Er and is shown in Fig. 2. In the frequency distribution curve of Er, there are two peaks centred around $1{\cdot}3\times10^{13}$ and $2{\cdot}1\times10^{13}$ Hz. There is a valley with a minimum around $1{\cdot}9\times10^{13}$ Hz. In the low-frequency region the distribution curve is parabolic according to the equation $g(\omega)=C\omega^2$. The constant C is determined from knowledge of the average value of $\sum_{j=1}^{3} V_j^{-3}(\theta,\varphi)$ where $V_j(\theta,\varphi)$ is the acoustic wave velocity of the jth mode propagating in the direction (θ,φ). The even moments (μ_2, μ_4, μ_6) of the frequency distribution function for Er on the present model have been calculated and are

$$\mu_2 = 2{\cdot}45\times10^{26}\ \mathrm{s}^{-2},$$
$$\mu_4 = 7{\cdot}48\times10^{52}\ \mathrm{s}^{-4},$$
$$\mu_6 = 25{\cdot}91\times10^{78}\ \mathrm{s}^{-6}. \qquad (3.8)$$

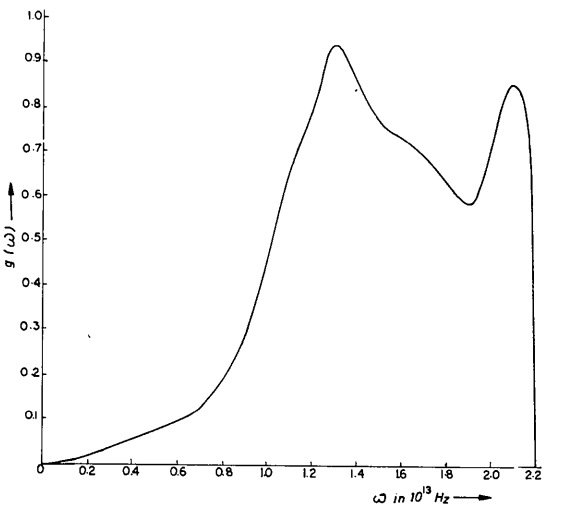

Fig. 2. Normalized frequency distribution function for erbium.

Table 2. *Wave velocities and generalized G.P.'s for the acoustic waves in erbium at different angles θ to the hexagonal axis*

The wave velocities and the G.P.'s are calculated using the SOE constants and the calculated TOE constants at 298 K. The velocities are in units of $10^{11/2}$ cm sec^{-1}.

θ^0	V_1	γ_1'	γ_1''	V_2	γ_2'	γ_2''	V_3	γ_3'	γ_3''
5	0·97	1·01	3·08	0·56	0·02	1·90	0·56	−0·03	1·95
15	0·97	0·95	3·05	0·57	0·37	1·50	0·56	0·06	1·80
25	0·96	0·89	2·94	0·58	0·90	0·91	0·56	0·22	1·51
35	0·96	0·88	2·68	0·59	1·34	0·45	0·56	0·43	1·13
45	0·95	1·01	2·20	0·59	1·47	0·36	0·56	0·68	0·69
55	0·96	1·28	1·55	0·59	1·23	0·67	0·56	0·92	0·25
65	0·96	1·62	0·89	0·58	0·74	1·20	0·56	1·13	−0·14
75	0·97	1·90	0·39	0·57	0·21	1·72	0·56	1·29	−0·43
85	0·98	2·05	0·12	0·56	−0·13	2·05	0·56	1·38	−0·59

The value of θ_∞, the high-temperature limit of the Debye temperature for Er as calculated from μ_2 has the value 154 K.

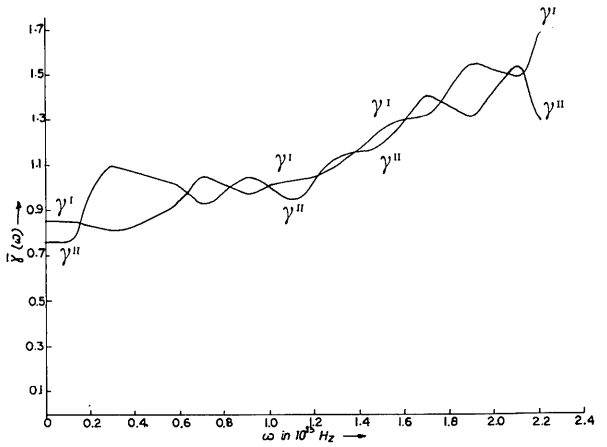

Fig. 3. $\bar{\gamma}'(\omega)$ and $\bar{\gamma}''(\omega)$ *versus* ω curves for erbium.

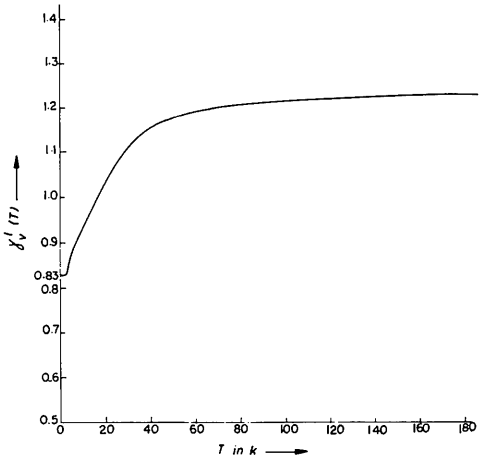

Fig. 4. $\bar{\gamma}_v^1(T)$ *versus* T curve for erbium.

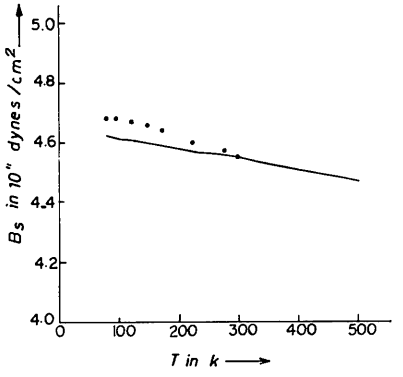

Fig. 5. Variation of bulk modulus of erbium with temperature. ● denotes experimental points.

The individual gammas γ' and γ'' for the various normal-mode frequencies in each frequency interval of width $\Delta\omega = 0{\cdot}2 \times 10^{13}$ Hz are noted and the average values $\bar{\gamma}'$ and $\bar{\gamma}''$ of these G.P.'s are calculated for each interval. The $\bar{\gamma}'(\omega)$ and $\bar{\gamma}''(\omega)$ *versus* ω curves are shown in Fig. 3. The effective Grüneisen functions $\bar{\gamma}_\perp^1(T)$ and $\bar{\gamma}_\parallel^1(T)$ at any temperature T are then evaluated from

$$\bar{\gamma}_\perp^1(T) = \frac{\int_0^{\omega_{max}} \bar{\gamma}'(\omega) g(\omega)\sigma(\omega, T)\mathrm{d}\omega}{\int_0^{\omega_{max}} g(\omega)\sigma(\omega, T)\mathrm{d}\omega},$$

$$\bar{\gamma}_\parallel^1(T) = \frac{\int_0^{\omega_{max}} \bar{\gamma}''(\omega) g(\omega)\sigma(\omega, T)\mathrm{d}\omega}{\int_0^{\omega_{max}} g(\omega)\sigma(\omega, T)\mathrm{d}\omega}, \qquad (3.9)$$

where $\sigma(\omega, T)$ is the Einstein specific heat function. The Brugger gammas at different temperatures are evaluated from (3.4) and hence the volume gamma as

$$\bar{\gamma}_v^1(T) = 2\bar{\gamma}_\perp^{Br}(T) + \bar{\gamma}_\parallel^{Br}(T). \qquad (3.10)$$

The variation of $\bar{\gamma}_v^1(T)$ with temperature is shown in Fig. 4. $\bar{\gamma}_v^1(T)$ increases rapidly up to 100 K; then becomes nearly flat and finally attains the high-temperature limit 1·23. This agrees well with the $\bar{\gamma}_H$ value, 1·17, from thermal data reported by Gschneidner (1964).

4. Anderson–Grüneisen parameter and bulk modulus of erbium

The Anderson–Grüneisen (A–G) parameter of Er has been calculated from its TOE constants obtained on the C.F. model using the procedure suggested by Ramji Rao (1974) and has the value 2·28. This agrees well with the value 2·31 obtained from the experimental pressure derivatives data of Er by the method indicated by Ramji Rao (1975*b*). From theoretical considerations Anderson (1966) derived the relation which gives the temperature dependence of the bulk modulus as a function of the specific heat and atomic volume V.

$$\frac{\mathrm{d}B_s}{\mathrm{d}T} = -\frac{\delta\gamma C_p}{V}. \qquad (4.1)$$

Here γ is the usual Grüneisen constant. The integrated form of B_s is then obtained as

$$B_s = B_{00} - \left(\frac{\delta\gamma}{V_0}\right)\int_0^T C_v\mathrm{d}T. \qquad (4.2)$$

B_{00} is the bulk modulus at absolute zero, V_0 is the specific volume per 'average' atom at 0 K and C_p is replaced by C_v. The theoretical curve showing the variation of the bulk modulus of Er with temperature is obtained from (4.2) and is shown in Fig. 5. $\int_0^T C_v\mathrm{d}T$

is the internal energy content of a solid at any temperature T and is tabulated (*American Institute of Physics Handbook*, 1963) as a function of temperature, knowing the characteristic temperature of the solid. The internal energy content of Er is obtained by treating it as a Debye solid. The values of the parameters V_0, ϱ, θ_D and B_{00} for Er are given in Table 3. The values of V_0, ϱ and θ_D correspond to those at room temperature. The agreement between the calculated B_s values and those obtained from the measured elastic constants (Fisher & Dever, 1967), at various temperatures up to 298 K, is good to within 2%.

Table 3. *Values of the constants of erbium used in the present calculations*

Debye temperature θ_D (K)	V_0	ϱ	B_{00} (10^{11} dynes cm^{-2})
191	18·45	9·064	4·63

5. Discussion

The close agreement between the calculated $\bar{\gamma}_H$ and the thermal $\bar{\gamma}_H$, the calculated and experimental A–G parameters and the calculated and experimental B_s values of Er amply justifies the use of the C.F. model to explain the thermal and mechanical properties of this rare-earth metal. The calculated pressure derivative $\partial C_{44}/\partial p$ is positive for Er, from which it may be inferred that the pressure-induced phase transformation from h.c.p. to b.c.c. structure is not possible in this metal. The G.P.'s in Er (both γ' and γ'') have small values, which is a characteristic feature of the h.c.p. rare-earth metals. The agreement of the frequencies of Er calculated on the C.F. model in the symmetry directions with the extrapolated frequencies is better than that obtained by Ramji Rao & Menon (1973) using Keating's (1966) approach.

One of us (A.R.) is grateful to the Council of Scientific and Industrial Research, Government of India for the award of a research fellowship.

References

American Institute of Physics Handbook (1963). 2nd ed. New York: McGraw-Hill.
ANDERSON, O. L. (1966). *Phys. Rev.* **144**, 553–557.
BLACKMAN, M. (1957). *Proc. Phys. Soc.* B**70**, 827–832.
BRUGGER, K. & FRITZ, T. C. (1967). *Phys. Rev.* (*A*), **157**, 524–531.
FISHER, E. S. & DEVER, D. (1967). *Trans. Metall. Soc. AIME*, **239**, 48–57.
FISHER, E. S., MANGHNANI, M. H. & KIKUTA, R. (1973). *J. Phys. Chem. Solids*, **34**, 687–703.
GLYDEN HOUMAN, J. C. & NICKLOW, R. M. (1970). *Phys. Rev.* (*B*), **1**, 3943–3952.
GSCHNEIDNER, K. A. JR (1964). *Solid State Phys.* **16**, 414.
KEATING, P. N. (1966). *Phys. Rev.* **145**, 637–645; **149**, 674–678.
NICKLOW, R. M., WAKABAYASHI, N. & VIJAYARAGHAVAN, P. R. (1971). *Phys. Rev.* (*B*), **3**, 1229–1234.
RAMJI RAO, R. (1974). *Phys. Rev.* (*B*), **10**, 4173–4177.
RAMJI RAO, R. (1975*a*). *Acta Cryst.* A**31**, 267–268.
RAMJI RAO, R. (1975*b*), *J. Phys. Soc. Japan*, **38**, 1080–1082.
RAMJI RAO, R. & MENON, C. S. (1973). *J. Appl. Phys.* **44**, 3892–3896.
RAMJI RAO, R. & SRINIVASAN, R. (1968). *Phys. Stat. Sol.* **29**, 865–871.
RAMJI RAO, R. & SRINIVASAN, R. (1970). *Proc. Indian Acad. Sci.* A**36**, 97–100.
RAMJI RAO, R. & SRINIVASAN, R. (1969). *Phys. Stat. Sol.* **31**, K 39–K 42.
SRINIVASAN, R. & RAMJI RAO, R. (1965). *Inelastic Scattering of Neutrons*, IAEA, Vienna, **1**, 325–342.

Acta Cryst. (1977). A**33**, 150–154

The Structure of $NaTaO_3$ by X-ray Powder Diffraction

BY M. AHTEE AND L. UNONIUS

Department of Physics, University of Helsinki, Helsinki, Finland

(*Received* 25 *June* 1976; *accepted* 30 *July* 1976)

The structure of $NaTaO_3$ has been determined from X-ray powder diffraction spectra by measuring the intensities of the difference reflexions caused by the deviations from the ideal cubic perovskite structure. The structure is compared with that determined on the basis of single-crystal measurements.

1. Introduction

In general, it is much easier to obtain a powder specimen than a truly untwinned single crystal. On the other hand, the powder method suits only the simplest structures because of the overlap of adjacent Bragg peaks in more complex structures. Rietveld (1969) has, however, developed a refinement method for neutron powder diffraction patterns. In this method the detailed shape of the powder pattern is used to decide between various structural models. This method is a structure refinement technique, *i.e.* the structure has already been solved approximately by X-ray or other techniques.

In this work, the structure of $NaTaO_3$ is determined by the X-ray diffraction powder method by making